Verweij JJ, Vermeer J, Brienen EAT, Blotkamp C, Laeijendecker D, Lieshout LV, Polderman AM (2003) *Entamoeba histolytica* infections in captive primates. Parasitol Res 90: 100-103

Legends to figures

Figure 1.

Schematic representation of polymorphism in the repeat-containing region of the chitinase gene among EHMfas1 and human isolates. Nucleotide sequences pattern (A) and deduced amino-acid sequences pattern (B) were shown. Each nucleotide sequence of unit was tentatively given a number. Nucleotide and deduced amino-acid sequences of these units are also shown. Enclosed units with bold line were EHMfas1-specific units. EHMfas1-specific mutations in nucleotide and deduced amino-acid sequences are underlined.

[a] EHMfas1-specific unit sequences.

Figure 2.

Schematic representation of polymorphism in the repeat-containing region of the SREHP gene among EHMfas1 and human isolates. Nucleotide sequences pattern (A) and deduced amino-acid sequences pattern (B) were shown. Each nucleotide and deduced amino-acid sequence of unit was tentatively given a number. Nucleotide and deduced amino-acid sequences of these units are also shown. Enclosed units with bold line were EHMfas1-specific units. EHMfas1-specific mutations in nucleotide and deduced amino-acid sequences are underlined.

[a] Minor unit sequences observed as strain-specific unit in some human isolates.

[b] EHMfas1-specific unit sequences.

[c, d, e] EHMfas1-specific block insertions, c: GAGGAA (EE), d: GATGAAGAA (DEE), e: GAGAAT (EN).

Figure 3.

Phylogenetic analysis of 16S-like SSUrDNA sequences among EHMfas1 and other *Entamoeba* species. Branch lengths are proportional to estimated number of substitutions per site, which represent the evolutional distance.

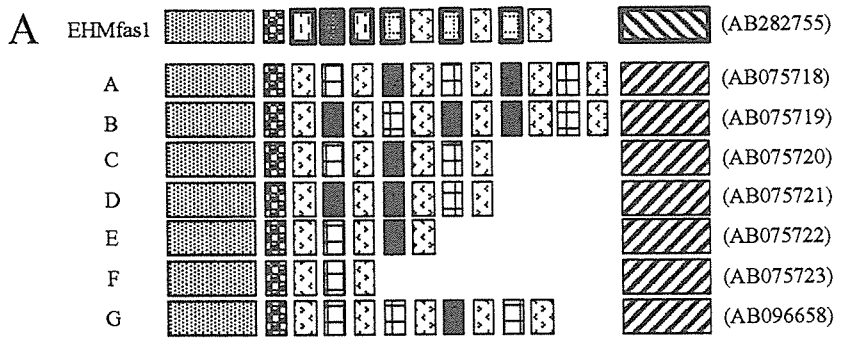

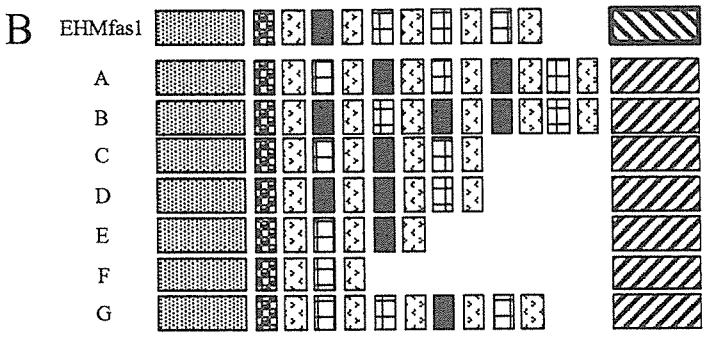

CN5 C ATATAACCCTTGTGTGTGGAATTTCCTTGACCTT
CCTGATTGTGAAAAAAAGCCAGGTGATTTCTTT

CN1 GAGAAGTCACCAGATTCTTCT

CN2 GAATCTAAACATGAATCTTCT

CN3 GAATCTAAGCATGAATCTTCT [a]

CN4 GAAATTAAACCAGATTCTTCT

CN5 GAAATTAAACCAGACTCTTCT [a]

CN6 GAAGTTAAACCAGATTCTTCT

CN7 GAAGTTAAACCAGACTCTTCT [a]

CN3 C1 GAGCCAGAAGTTAGTATCCCAAAGAAAACAGT
TGCTTATTATACTAATTGGGCACAATACAGA

CN3 C2 GAGCCAGAAGTTAGTGTCCCAAAGAAAACAGT
TGCTTATTATACTAATTGGGCACAATACAGA [a]

CA5 C YNPCVWNFLDLPDCEKKPGDFF

CA1 EKSPDSS

CA2 ESKHESS

CA3 EIKPDSS

CA4 EVKPDSS

CA3 C1 EPEVSIPKKTVAYYTNWAQYR

CA3 C2 EPEVSVPKKTVAYYTNWAQYR [a]

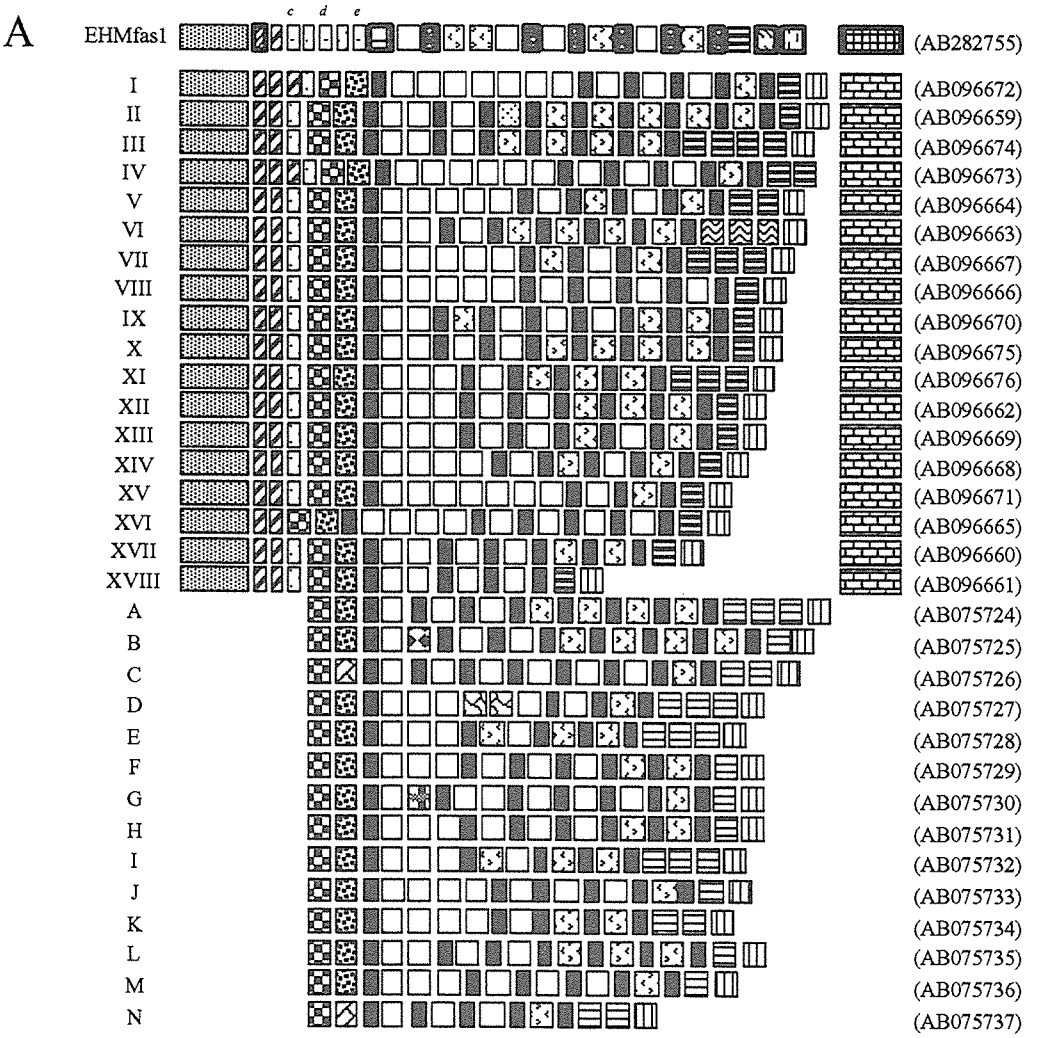

SN5 C GAAAAAGAAAAAAGTAGCTCAGCAAA ACCAGAATCAAGTTCA

SN1 AATGAAGAT
SN2 AACAAAGAT[b]

SN5 GATGAAGAT

SN4 GAAAAAGCAAGTTCAAGTGATAACTCA
SN5 GAAAAAGCAAGTTCAAGTGATAATCA[b]

SN6 GAATCAAGCTCAAGTGATAAACCA

SN7 GAATCAAGTTCAAGTGATAAACCA[a]

SN8 GATAATAAACCA
SN9 GATAACAAACCA[b]

SN10 GAAGCAAGTTCAAGTGATAAACCA

SN11 GAAGCAAGCTCAAGTGATAAACCA

SN12 GAAGCTAGTTCAAGTGATAAACCA[a]

SN13 GAAGCAAGTTCAAGTGATAAATCA[a]

SN14 GAAGCAAGTTCAAGTGATAATCCA[a]

SN15 GAAGCAAGTTCAAGTGAAAGTCCA[a]

SN16 GAAGCAAGCTCAACTAATAAACCA
SN17 GAAGCAAGTTCAACTAATAAACCA[b]

SN18 GAAGCAAGCTCAACTGATAAACCA[a]

SN19 GAAGCAAGCTCAACTAGTAATTCA
SN20 GAAGCAAGTTCAACTAGTAATTCA[b]

SN3 C1 AATGATAAATCAGGAAGTAGTTCA GATAACGATAATAAT

SN3 C2 AATGATAAATCAGAAAGTAGTTCA GATAATGATAATAAT[b]

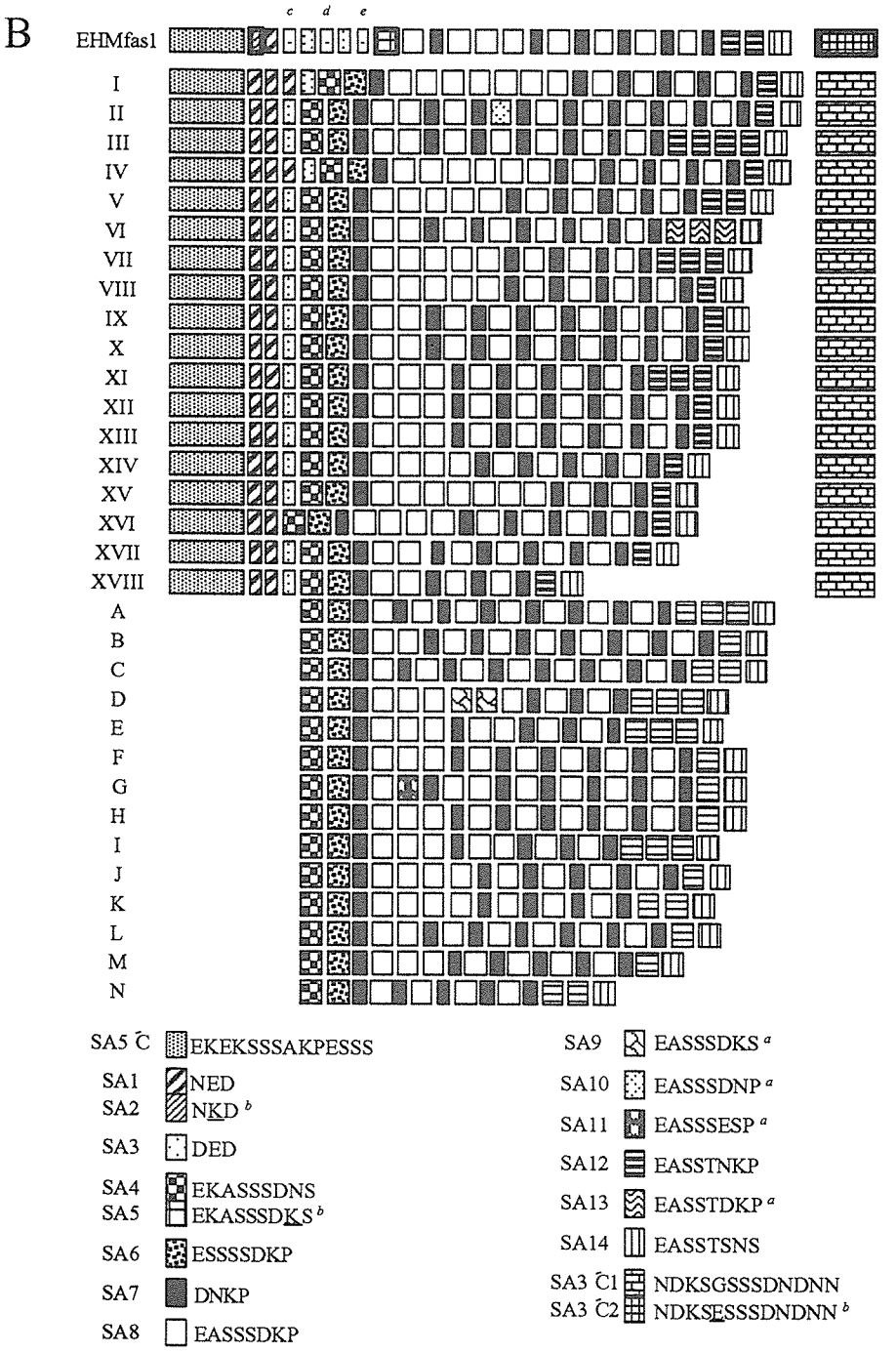
B
c
d
e
EHMfas1
I
II
III
IV
V
VI
VII
VIII
IX
X
XI
XII
XIII
XIV
XV
XVI
XVII
XVIII
A
B
C
D
E
F
G
H
I
J
K
L
M
N
SA5 C̆ EKEKSSSAKPESSS
SA1 NED
SA2 NKD b
SA3 DED
SA4 EKASSSDNS
SA5 EKASSSDKS b
SA6 ESSSSDKP
SA7 DNKP
SA8 EASSSDKP
SA9 EASSSDKS a
SA10 EASSSDNP a
SA11 EASSSESP a
SA12 EASSTNKP
SA13 EASSTDKP a
SA14 EASSTSNS
SA3 C̆1 NDKSGSSSDNDNN
SA3 C̆2 NDKSESSSDNDNN b

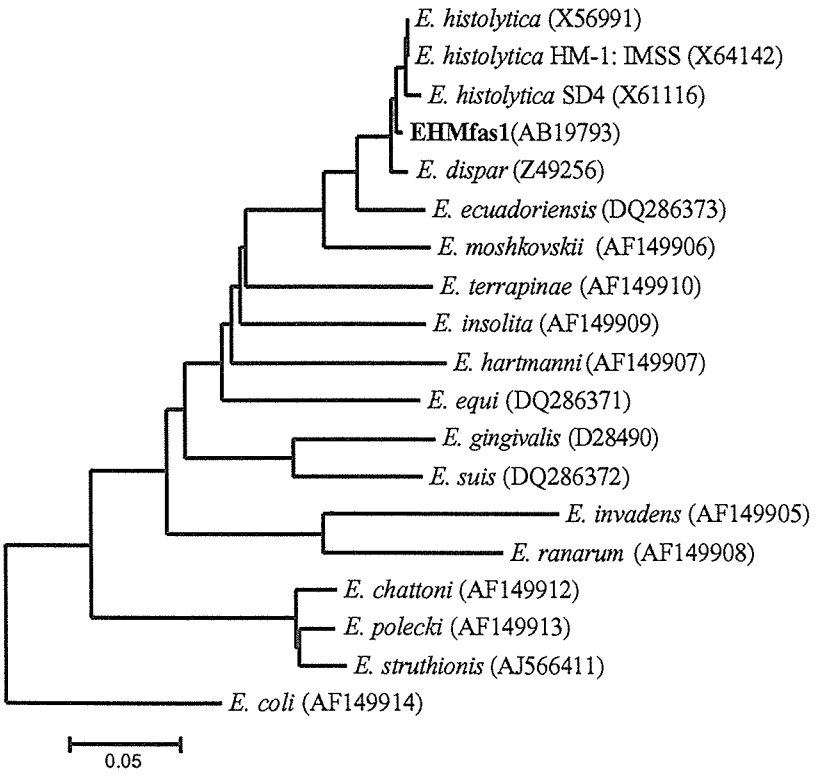
E. histolytica (X56991)
E. histolytica HM-1: IMSS (X64142)
E. histolytica SD4 (X61116)
EHMfas1(AB19793)
E. dispar (Z49256)
E. ecuadoriensis (DQ286373)
E. moshkovskii (AF149906)
E. terrapinae (AF149910)
E. insolita (AF149909)
E. hartmanni (AF149907)
E. equi (DQ286371)
E. gingivalis (D28490)
E. suis (DQ286372)
E. invadens (AF149905)
E. ranarum (AF149908)
E. chattoni (AF149912)
E. polecki (AF149913)
E. struthionis (AJ566411)
E. coli (AF149914)
0.05

Parasitol Res (2006) 98: 443–446
DOI 10.1007/s00436-005-0025-7

ORIGINAL PAPER

Asao Makioka · Masahiro Kumagai · Seiki Kobayashi · Tsutomu Takeuchi

Effect of artificial gastrointestinal fluids on the excystation and metacystic development of *Entamoeba invadens*

Received: 5 May 2005 / Accepted: 20 September 2005 / Published online: 14 January 2006

Abstract The effect of artificial gastric fluid (AGF), containing 0.5% pepsin and 0.6% hydrochloric acid, pH 1.8, in distilled water, on the excystation and metacystic development of *Entamoeba invadens* was examined. Excystation, which was assessed by counting the number of metacystic amoebae after inducing excystation, was enhanced by pretreatment of cysts with AGF for 30 to 60 min at 37°C but not 26°C. Longer exposure of cysts to AGF significantly reduced their viability. Significant enhancement of excystation was observed by pretreatment of cysts with distilled water only at 37°C. In addition, 0.6% hydrochloric acid had a comparable enhancing effect on excystation to AGF. Metacystic development, when determined by the number of nuclei in amoeba, was slightly enhanced by pretreatment with AGF. An artificial intestinal fluid (AIF), containing 1% pancreatin, 1% sodium bicarbonate, and 5% ox bile, pH 8.0, in distilled water, had a significant toxic effect on cysts, where 1% pancreatin had neither an enhancing effect on excystation nor a toxic effect on cysts, whereas 5% ox bile had a toxic effect on cysts. Pretreatment of cysts with AGF followed by AIF had a similar toxic effect on cysts to that by AIF only. These results suggest that gastric fluid but not intestinal fluid at 37°C contributes to enhancing excystation for *Entamoeba* infection.

A. Makioka (✉) · M. Kumagai
Department of Tropical Medicine,
Jikei University School of Medicine,
3-25-8 Nishi-shinbashi, Minato-ku,
Tokyo 105-8461, Japan
e-mail: makioka@jikei.ac.jp
Tel.: +81-3-34331111
Fax: +81-3-34314459

S. Kobayashi · T. Takeuchi
Department of Tropical Medicine and Parasitology,
Keio University School of Medicine,
35 Shinanomachi, Shinjuku-ku,
Tokyo 160-8582, Japan

Introduction

Following the ingestion of cysts in contaminated food or water, excystation and metacystic developments are essential for *Entamoeba* infection, and their processes have been described for *Entamoeba histolytica* (Dobell 1928; Cleveland and Sanders 1930). Since *E. histolytica* does not encyst efficiently in axenic cultures, *Entamoeba invadens*, a reptilian parasite, has been commonly accepted as a model for the study of encystation and excystation (López-Romero and Villagómez-Castro 1993; Eichinger 1997). Excystation is the process through which the whole organism escapes from the cyst through a minute perforation in the cyst wall. Metacystic development is the process in which a hatched metacystic amoeba with four nuclei divides to produce eight amoebulae, which grow to become trophozoites (Dobell 1928; Cleveland and Sanders 1930; Geiman and Ratcliffe 1936). The transfer of *E. invadens* cysts in an encystation medium to a growth medium induces in vitro excystation (McConnachie 1955; Rengpien and Bailey 1975; Garcia-Zapien et al. 1995; Makioka et al. 2002). Before excystation in the ileum, cysts are exposed to gastric fluid and then intestinal fluid during passage through the stomach and intestine. Although cysts are resistant to gastric fluid, there are no reports of the effect of gastrointestinal fluid on the excystation and metacystic development of *Entamoeba*. We examined the effect of artificial gastrointestinal fluid on these processes of *E. invadens*. Here, we report that artificial gastric fluid (AGF) enhances excystation but has little effect on metacystic development, while artificial intestinal fluid (AIF) had a significant toxic effect on cysts, which was due to the bile in the fluid.

Materials and methods

Trophozoites of *E.invadens* strain IP-1 were cultured in an axenic growth medium BI-S-33 (Diamond et al. 1978) at 26°C. To obtain cysts, trophozoites (5×10^5 cells/ml) were transferred to an encystation medium called 47% LG (LG is BI without glucose; Sanchez et al. 1994). After 3 days of incubation, the percentage of encystation reached 80% on

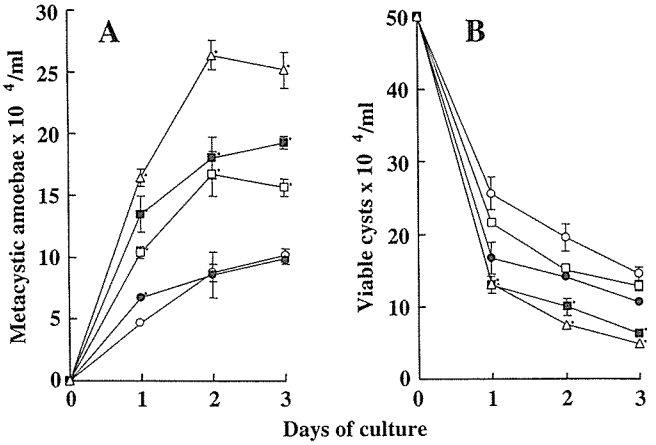

Fig. 1 Effect of AGF on the number of metacystic amoebae (**a**) and viable cysts (**b**) of *E. invadens*. The cysts were transferred to a growth medium without (*open circles*) or after pretreatment at 37°C with distilled water for 30 min (*filled circles*) or 60 min (*filled squares*) and with AGF for 30 min (*open squares*) or 60 min (*open triangles*). The mean numbers±SE of metacystic amoebae or viable cysts for duplicate cultures are plotted (each *asterisk* indicates $P<0.05$)

average. The cells were harvested and treated with 0.05% sarkosyl (Sigma Chemical Co., St. Louis, MO, USA) to destroy the trophozoites (Sanchez et al. 1994). The remaining cysts were washed with phosphate-buffered saline and counted. The viability of the cysts was determined by trypan blue dye exclusion, and the number of nuclei per cyst was determined after staining with modified Kohn's stain (Kumagai et al. 2001). Cyst preparation included 30% dead or denatured cysts and 70% viable cysts, where four-nucleate cysts are 30% and one- to three-nucleate cysts are 70%. For the experiments on excystation, cysts (5×10^5 cells/ml) in duplicate were suspended in a growth medium and were incubated for 3 days in the controls. For the experiments on the effect of AGF containing 0.5% pepsin (Nacalai Tesque, Kyoto, Japan) and 0.6% hydrochloric acid, pH 1.8, in distilled water on excystation, cysts were exposed to AGF for 30 or 60 min at 37°C, washed twice in the growth medium by centrifugation, and then suspended in a fresh growth medium, unless otherwise specified. Metacystic amoebae were counted in a hemocytometer on days 1 and 3, and their viability was determined by trypan blue dye exclusion. Viable metacystic amoebae and cysts were clearly distinguished as pale yellow and light blue in color, respectively. The former was also identified by positive motility. Metacystic development was determined by the number of nuclei per amoeba. The cells were harvested on days 1 and 3 in cultures and stained with modified Kohn's stain. The number of nuclei per amoeba was determined by the double counting of least 100 amoebae. A solution containing 1% pancreatin (Nacalai), 1% sodium bicarbonate, and 5% ox bile (Sigma), pH 8.0, in distilled water was used as the AIF (Heath and Smith 1970). For the experiments on the effect of AIF on excystation, the cysts were exposed to AIF for 60 min at 37°C, washed twice in a growth medium by centrifugation, and suspended in a fresh growth medium. For the combined effect of AGF and AIF on excystation, the cysts were exposed first to AGF for 60 min at 37°C, sedimented by centrifugation to remove AGF, and then exposed to AIF for 60 min at 37°C before transfer to the growth medium.

All experiments were performed at least three times, and similar results were obtained in each replicate. Therefore, representative data from duplicate cultures are shown in the results.

Results and discussion

Effect of AGF on excystation and viability of cysts

The effect of pretreatment of cysts with AGF on the number of metacystic amoebae and viable cysts of *E. invadens* before transfer to the growth medium is shown in Fig. 1a. The number of metacystic amoebae in cultures of cysts pretreated for 30 min with AGF during incubation increased compared to the controls. Pretreatment with distilled water for 30 min also increased the number of amoebae compared to the controls. When the pretreatment was increased from 30 to 60 min, metacystic amoebae further increased in number by pretreatment with AGF and distilled water. The effect of AGF on cyst viability is shown in Fig. 1b. The number of viable cysts in the control cultures decreased during incubation. It is considered that most immature cysts contained in culture degenerate or die

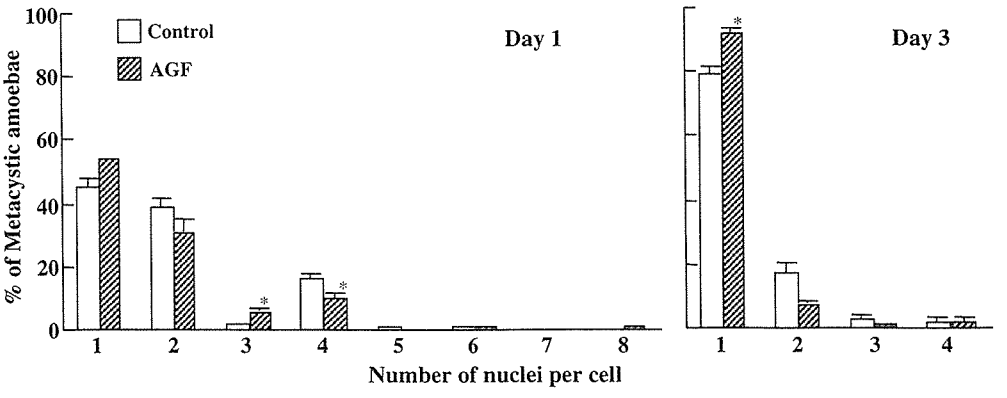

Fig. 2 Effect of AGF on the metacystic development of *E. invadens*. The cysts were transferred to a growth medium without or after pretreatment at 37°C with AGF for 60 min. The number of nuclei per metacystic amoeba stained with modified Kohn on days 1 and 3 of incubation was counted, and the percentage of amoebae in each class (1- to 8-nucleate) was determined (each *asterisk* indicates $P<0.05$)

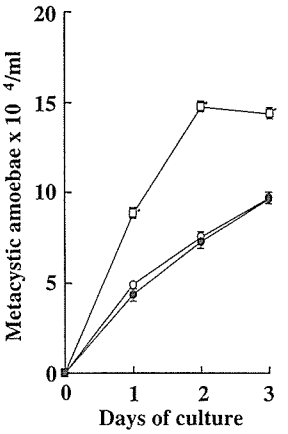

Fig. 3 Effect of temperature of pretreatment on the number of metacystic amoebae of *E. invadens*. The cysts were transferred to a growth medium without (*open circles*) or after pretreatment at 26°C (*filled circles*) or 37°C (*open squares*) with AGF for 60 min. The mean numbers±SE of metacystic amoebae for duplicate cultures are plotted (each *asterisk* indicates $P<0.05$)

during incubation. The number of viable cysts in cultures of cysts pretreated with AGF or distilled water for 30 min during incubation was comparable to that of the controls, whereas pretreatment with AGF for 60 min reduced the number of viable cysts compared to the controls. This suggests that longer exposure to AGF had a detrimental effect on the cysts.

Effect of AGF on metacystic development

The effect of AGF on metacystic development was examined by counting the number of nuclei per cell. As shown in Fig. 2, 16 and 83% of the metacystic amoebae were four-nucleate and one- to three-nucleate, respectively, on day 1 of incubation in the control cultures, whereas 11 and 89% of amoebae, respectively, were in cultures of cysts pretreated with AGF. The percentage of four-nucleate amoebae in the control cultures then decreased to 2%, and that of 1-nucleate amoeba increased to 79% on day 3, while the percentages were 2 and 92%, respectively, in cultures of cysts pretreated with AGF, suggesting a small enhancing effect on metacystic development by pretreatment with AGF.

Effect of temperature of pretreatment with AGF on excystation

The effect of temperature of pretreatment with AGF on excystation is shown in Fig. 3. No increase in the number

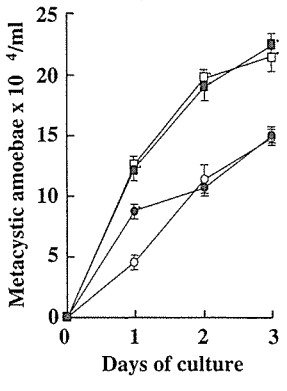

Fig. 4 Comparison of effect of pepsin, hydrochloric acid, and AGF on the number of metacystic amoebae of *E. invadens*. The cysts were transferred to a growth medium without (*open circles*) or after pretreatment for 60 min at 37°C with 0.5% pepsin in distilled water (*filled-circles*), 0.6% hydrochloric acid (*open squares*), or AGF (*filled squares*). The mean numbers± SE of metacystic amoebae for duplicate cultures are plotted (each *asterisk* indicates $P<0.05$)

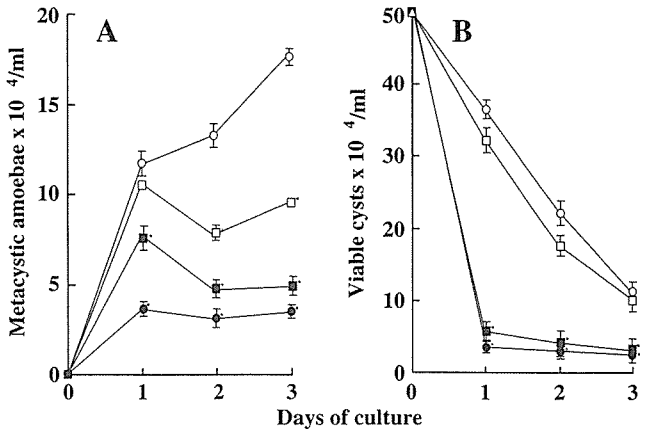

Fig. 5 Effect of AIF on the number of metacystic amoebae (**a**) and viable cysts (**b**) of *E. invadens*. The cysts were transferred to a growth medium without (*open circles*) or after pretreatment with AIF (*filled circles*), 1% pancreatin (*open squares*), or 5% bile (*filled squares*) for 60 min at 37°C. The mean numbers±SE of metacystic amoebae and viable cysts for duplicate cultures are plotted (each *asterisk* indicates $P<0.05$)

of metacystic amoebae by pretreatment of cysts with AGF at 26°C occurred, unlike at 37°C, indicating that a higher temperature of 37°C is critical for this effect. The results can be applied to excystation of the human parasite, *E. histolytica*, but are unlikely to be applicable to that of *E. invadens* in reptiles. Although encystation and excystation of *E. invadens* are important as models of encystation and excystation of *E. histolytica*, the difference in temperature for the axenic growth of the two species is definitive so that it is unlikely that temperature plays an important role in the in vivo excystation of *E. invadens*.

Comparison of effect of pepsin, hydrochloric acid, and AGF on excystation

The effect of pepsin in distilled water, hydrochloric acid, and AGF on excystation was compared. As shown in Fig. 4, the increase in the number of metacystic amoebae by pretreatment with 0.6% hydrochloric acid was very similar to that

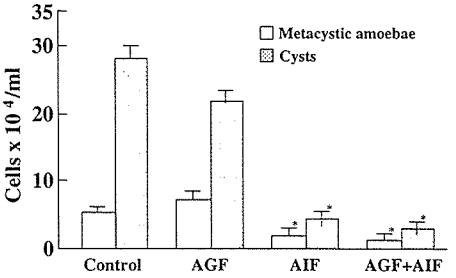

Fig. 6 Combined effect of AGF and AIF on the number of metacystic amoebae and viable cysts. The cysts were transferred to a growth medium without or after pretreatment with AGF or with AGF + AIF. The mean numbers±SE of metacystic amoebae and viable cysts on day 1 for duplicate cultures are plotted (each *asterisk* indicates $P<0.05$)

with AGF compared to the controls, whereas the increase occurred to a lesser extent only on day 1 by pretreatment with 0.5% pepsin in distilled water. This suggests that acidic conditions are important for the enhancing effect on excystation. Similar results were reported on *Giardia* in which excystation of this parasite could be induced by acidic solutions and also that salts and pepsin did not significantly alter the level of excystation in these solutions (Bingham and Meyer 1979). The mechanism for induction of *Giardia* and *Entamoeba* excystation by acidic conditions is unclear.

Effect of AIF on excystation and viability of cysts

The effect of pretreatment of cysts with AIF on the number of metacystic amoebae and viable cysts is shown in Fig. 5. Pretreatment of cysts with AIF for 60 min at 37°C significantly reduced the number of viable cysts, and few metacystic amoebae appeared. Similar results were obtained with exposure to AIF for 30 min (data not shown). When the effect of 1% pancreatin was compared with that of 5% ox bile, pancreatin showed neither an enhancing effect nor a toxic effect on cysts, whereas ox bile showed a toxic effect on cysts, indicating that the toxic effect on cysts by AIF was due to the bile.

Combined effect of AGF and AIF on excystation and viability of cysts

The effect of AGF and AIF on the number of metacystic amoebae and viable cysts on day 1 of incubation is shown in Fig. 6. Exposure of cysts to AGF and AIF resulted in a significant reduction in the number of viable cysts and little emergence of metacystic amoebae, which was similar to the results of AIF only.

In summary, these results suggest that gastric fluid but not intestinal fluid at 37°C contributes to enhancing excystation for *Entamoeba* infection.

Acknowledgements We thank Dr. N. Watanabe for valuable discussion, Dr. L.S. Diamond for supplying the *E. invadens*, and T. Tadano for technical assistance. This work was supported by a Grant-in-Aid for Scientific Research from the Ministry of Education, Culture, Sports and Technology of Japan and by a Health Science Research Grant for Research on Emerging and Re-emerging Infectious Diseases from the Ministry of Health, Labor and Welfare of Japan.

References

Bingham AK, Meyer EA (1979) *Giardia* excystation can be induced in vitro in acidic solutions. Nature 277:301–302

Cleveland LR, Sanders EP (1930) Encystation, multiple fission without encystment, excystation, metacystic development, and variation in a pure line and nine strains of *Entamoeba histolytica*. Arch Protistenkd 70:223–266

Diamond LS, Harlow DR, Cunnick CC (1978) A new medium for the axenic cultivation of *Entamoeba histolytica* and other *Entamoeba*. Trans R Soc Trop Med Hyg 72:431–432

Dobell C (1928) Researches on the intestinal protozoa of monkeys and man. Parasitology 20:357–412

Eichinger D (1997) Encystation of *Entamoeba* parasites. Bioessays 19:633–639

Garcia-Zapien A, Hernandez-Gutierrez R, Mora-Galindo J (1995) Simultaneous growth and mass encystation of *Entamoeba invadens* under axenic conditions. Arch Med Res 26:257–262

Geiman QM, Ratcliffe HL (1936) Morphology and life-cycle of an amoeba producing amoebiasis in reptiles. Parasitology 28:208–230

Heath DD, Smith JD (1970) In vitro cultivation of *Echinococcus granulosus*, *Taenia hydatigena*, *T. pisiformis* and *T. serialis* from oncosphere to cystic larva. Parasitology 61:329–343

Kumagai M, Kobayashi S, Okita T, Ohtomo H (2001) Modifications of Kohn's chlorazol black E staining and Wheatley's trichrome staining for temporary wet mount and permanent preparation of *Entamoeba histolytica*. J Parasitol 87:701–704

López-Romero E, Villagómez-Castro JC (1993) Encystation in *Entamoeba invadens*. Parasitol Today 9:225–227

Makioka A, Kumagai M, Ohtomo H, Kobayashi S, Takeuchi T (2002) Effect of proteasome inhibitors on the growth, encystation, and excystation of *Entamoeba histolytica* and *Entamoeba invadens*. Parasitol Res 88:454–459

McConnachie EW (1955) Studies on *Entamoeba invadens* Rodhain, 1934, in vitro, and its relationship to some other species of *Entamoeba*. Parasitology 45:452–481

Rengpien S, Bailey GB (1975) Differentiation of *Entamoeba*: a new medium and optimal conditions for axenic encystation of *E. invadens*. J Parasitol 61:24–30

Sanchez L, Enea V, Eichinger D (1994) Identification of a developmentally regulated transcript expressed during encystation of *Entamoeba invadens*. Mol Biochem Parasitol 67:125–135

Available online at www.sciencedirect.com
SCIENCE DIRECT
ELSEVIER
Molecular & Biochemical Parasitology 145 (2006) 216–225
MOLECULAR & BIOCHEMICAL PARASITOLOGY

Characterization of protein geranylgeranyltransferase I from the enteric protist *Entamoeba histolytica*☆

Asao Makioka[a], Masahiro Kumagai[a], Tsutomu Takeuchi[b], Tomoyoshi Nozaki[c,d,*]

[a] *Department of Tropical Medicine, Jikei University School of Medicine, 3-25-8 Nishi-shinbashi, Minato-ku, Tokyo 105-8461, Japan*
[b] *Department of Tropical Medicine and Parasitology, Keio University School of Medicine, 35 Shinanomachi, Shinjuku-ku, Tokyo 160-8582, Japan*
[c] *Department of Parasitology, Gunma University Graduate School of Medicine, 3-39-22 Showa-machi, Maebashi, Gunma 371-8511, Japan*
[d] *Precursory Research for Embryonic Science and Technology, Japan Science and Technology Agency, 2-20-5 Akebonocho, Tachikawa, Tokyo 190-0012, Japan*

Received 23 August 2005; received in revised form 28 September 2005; accepted 4 October 2005
Available online 19 October 2005

Abstract

Entamoeba histolytica is a unique protozoan parasite possessing both protein farnesyltransferase and geranylgeranyltrasferase I (GGT-I) for isoprenylation of small GTPases. In this study, we demonstrated unique enzymological properties of the amebic GGT-I (*Eh*GGT-I), including substrate specificity and insensitivity to known mammalian inhibitors. Some of important residues of the catalytic β subunit implicated in the specificity for GTPase acceptors and prenyl donors are substituted in *Eh*GGT-I. Recombinant α and β subunits of *Eh*GGT-I, co-expressed in *Escherichia coli*, showed activity to transfer geranylgeranyl to both human wild-type (CVLS) and mutant (CVLL) H-Ras, while the mammalian GGT-I geranylgeranylated, but not farnesylated, only mutant H-Ras. All the representative amebic Ras and Rho/Rac small GTPases with phenylalanine, leucine, methionine, or alanine terminus were preferentially geranylgeranylated by *Eh*GGT-I. This indicates that the acceptor specificity of the amebic GGT-I is remarkably broader than that of its mammalian counterpart. In contrast to *Eh*FT, which farnesylates but not geranylgeranlylates solely *Eh*Ras4-CVVA, *Eh*GGT-I also showed significant farnesyltransferase activity against Ras GTPase acceptors. *Eh*GGT-I showed remarkable resistance to peptidomimetics known to inhibit mammalian GGT-I. Together with our previous observation that this parasite does not appear to depend on farnesylation for a majority of Ras and Rho/Rac, these data indicate that biological and biochemical advantages leading to the evolutional selection of this isoprenyl modification must exist uniquely in this parasitic protist. Finally, remarkable biochemical differences in binding to substrates and inhibitors between amebic and mammalian GGT-I highlight this enzyme as an attractive target for the development of new chemotherapeutics against amebiasis.

Keywords: *Entamoeba histolytica*; Protein prenylation; Protein geranylgeranyltransferase I; Protein farnesyltransferase; Ras superfamily small GTPases

1. Introduction

Protein geranylgeranyltransferase type I (GGT-I; E.C. 2.5.1.59) and a closely related protein, farnesyltransferase (FT), are prenyl enzymes responsible for geranylgeranylation and farnesylation, respectively, which are major posttranslational lipid modifications of proteins including small GTPases of the Ras superfamily [1]. The isoprenylation of small GTPases is required for membrane association and their function in signal transduction involved in cell proliferation, differentiation and intracellular membrane trafficking [1–3]. GGT-I and FT, which are also called as CaaX prenyltransferases [4], catalyze

Abbreviations: GGT-I, protein geranylgeranyltrasferase I; *Eh*GGT-I, *Entamoeba histolytica* GGT-I; FT, protein farnesyltransferase; GGPP, geranylgeranyl pyrophosphate; FPP, farnesyl pyrophosphate; GGT-Iα, α subunit of GGT-I; GGT-Iβ, β subunit of GGT-I; SDS-PAGE, sodium dodecyl sulfate-polyacrylamide gel electrophoresis; NTA, Ni-nitrilotriacetic acid

☆ *Note:* The nucleotide sequence data of *Entamoeba histolytica* GGT-Iβ reported in this paper has been submitted to the DDBJ/GenBank®/EBI data bank with Accession number AB161971.

* Corresponding author. Tel.: +81 27 220 8020; fax: +81 27 220 8025.
E-mail address: nozaki@med.gunma-u.ac.jp (T. Nozaki).

0166-6851/$ – see front matter © 2005 Elsevier B.V. All rights reserved.
doi:10.1016/j.molbiopara.2005.10.005

the transfer of the geranylgeranyl and farnesyl group from geranylgeranyl pyrophosphate (GGPP) and farnesyl pyrophosphate (FPP), respectively, to the cysteine residue of a carboxyl-terminal CaaX of small GTPases including Ras, Rac, Rho, and Rap, where C, a, or X is cysteine, an aliphatic amino acid, or any amino acid, respectively. Mammalian FT or GGT-I generally prefers substrates including small GTPases possessing a terminal CaaX, where X is one of the following amino acids: Cys, Ser, Gln, Ala, Met, Thr, His, Val, Asn, Phe, Gly, or Ile for FT and Leu, Phe, Ile, Val, or Met for GGT-I in the order of decreasing affinity [5]. However, exceptions have been described in various organisms: e.g. K-RasB-CVIM is isoprenylated by both FT and GGT-I [6]. These data suggest the presence of not-yet-identified mechanistic details determining the substrate preferences of these isoprenyl enzymes. The third enzyme, GGT-II, transfers the geranylgeranyl groups from GGPP to both cysteine residues of CC- or CXC-containing proteins almost exclusively composed of members of the Rab family small GTPases [1].

Mutations in Ras, which correlate with cellular transformation and tumor development, have been found in nearly 30% of all human cancers [7]. Oncogenic Ras proteins have been shown to require farnesylation for their ability to transform cells [1]. Consequently, FT has been attracting attention as a target of cancer chemotherapy [8]. FT inhibitors have also been found to be effective against parasitic infections such as African sleeping sickness caused by *Trypanosoma brucei* and malaria caused by *Plasmodia* species [9]. Although GGT-I has drawn less attention than FT, GGT-I inhibitors are also viewed as potential anticancer agents because K-RasB, the most commonly mutated form of Ras, has often been shown to be geranylgeranylated as well as farnesylated [6]. Furthermore, a number of studies have shown that GGT-I inhibitors are effective against tumor progression [10] and smooth muscle hyperplasia [11].

Entamoeba histolytica is the intestinal protozoan parasite that causes amebic dysentery, colitis, and liver abscess in humans, and is responsible for an estimated 50 million cases of amebiasis and 40–100 thousand deaths annually [12]. A number of small GTPases of this parasite have been studied including Ras/Rap [13,14], Rho/Rac [15–19], and Rab [20–23], and the molecular and cellular functions of some of these small GTPases are beginning to be unveiled [13,18,19,23–25]. To elucidate the prenylation of these small GTPases in *E. histolytica*, we previously cloned genes encoding the α- and β-subunits of FT of this parasite and characterized the FT recombinant enzyme, which revealed remarkable biochemical differences in binding to substrates and inhibitors from mammalian FT [26]. We showed that the amebic FT did not utilize a majority of Ras and Rap as a substrate, but specifically farnesylated only a single Ras isotype, Ras4, which possesses an unusual primary structure. However, the molecular and biochemical identity of an enzyme (or enzymes) responsible for the isoprenylation of the remaining Ras and Rap proteins in this organism remains unknown.

To better understand the peculiarity of substrate selection of isoprenylation enzymes in this parasitic protozoon, we characterized GGT-I from *E. histolytica* (*Eh*GGT-I) in this study. We show that *Eh*GGT-I exhibits activity against a wide spectrum of small GTPases of *E. histolytica*, which is in marked contrast to *Eh*FT. We also show remarkable differences in substrate specificity and sensitivity against known peptidomimetic inhibitors of mammalian GGT-I between *Eh*GGT-I and rat GGT-I, indicating amebic GGT-I to be an ideal target for the development of new chemotherapeutics against amebiasis.

2. Materials and methods

2.1. Parasite

Trophozoites of *E. histolytica* strain HM:IMSS cl6 [27] were cultured axenically in BI-S-33 medium at 35.5 °C [28].

2.2. Chemicals

Recombinant rat GGT-I, recombinant human H-Ras-CVLS (wild type), H-Ras-CVLL (mutant), and peptidomimetic inhibitors GGTI-287 (*N*-4-[2 (*R*)-amino-3-mercatopropyl] amino-2-phenylbenzoyl-(L)-leucine trifluoroacetate) and GGTI-297 (*N*-4-[2(*R*)-amino-3-mercatopropyl]amino-2-naphthylbenzoyl-(L)-leucine trifluoroacetate) were purchased from EMD Biosciences (La Jolla, CA). [^{3}H] geranylgeranyl pyrophosphate (23.0 Ci/mmol) and [^{3}H] farnesyl pyrophosphate (16.1 Ci/mmol) were purchased from Perkin-Elmer Life Sciences (Boston, MA). Restriction endonucleases and modifying enzymes were purchased from Takara Biochemical (Tokyo, Japan). The other chemicals and reagents were purchased from either Sigma–Aldrich Fine Chemicals (St. Louis, MO) or Wako Pure Chemical Industries (Osaka, Japan) unless otherwise mentioned and were of the highest purity available.

2.3. cDNA library of E. histolytica

A trophozoite cDNA library of *E. histolytica* was constructed using the poly(A)$^+$ RNA and λZAP II phage (Stratagene, La Jolla, CA) as described previously [29].

2.4. Identification and cloning of GGT-Iβ of E. histolytica

We designed oligonucleotide primers to amplify the protein-coding region of the GGT-I β subunit from *E. histolytica* by PCR based on a homology search using yeast and mammalian GGT-I against the *E. histolytica* genome database available at The Institute for Genomic Research (http://www.tigr.org/tdb/). The sense and antisense primers for *Eh*GGT-Iβ were 5′-ATGAATGCACCTAATTTAAGAAGTGAAG-3′ and 5′-TCAAAGATATGATGGTTTTTCAATTCC-3′, respectively. PCR was performed using a one-hundredth volume of the cDNA phage lysate as a template with the following parameters. The initial step of denaturation at 94 °C for 3 min was followed by 30 cycles of denaturation at 94 °C for 1 min, annealing at 55 °C for 2 min, and extension at 72 °C for 2 min. The final step at 72 °C for 10 min was added to complete the extension. The amplified DNA fragments were electrophoresed, purified using a Geneclean II kit (BIO101, La Jolla, CA) and used as templates for subsequent PCR (see below). Since FT and GGT-I share their α subunit in all the organisms so far analyzed, we utilized the α subunit of

E. histolytica FT [26] as the GGT-I α subunit. Thus, the term "GGT-I α subunit" is synonymous with "FT α subunit" in this study. The nucleotide sequences reported in this paper have been submitted to the DDBJ/GenBank™/EBI Data Bank with accession number AB161971 (GGT-Iβ of *E. histolytica*).

2.5. Construction of a plasmid to express recombinant EhGGT-I

A plasmid containing the protein-coding regions of GGT-Iα (without the stop codon), GGT-Iβ (with the stop codon), and the ribosome-binding sequence (GAGGAGTTTTAACTT) between them was constructed by three rounds of PCR [30,31]. Briefly, a set of initial-round PCRs were conducted to amplify the GGT-Iα and GGT-Iβ protein-coding region using a sense primer, 5′-ATGGAAGAAGACGAAGAAATCACATTTG-3′, and an antisense primer, 5′-ATGATTAGTAATTTTTGTTAAATACCAATCCC-3′ (for GGT-Iα), and using a sense primer, 5′-ATGAATGCACCTAATTTAAGAAGTGAAG-3′, and an antisense primer, 5′-TCAAAGATATGATGGTTTTTCAATTCC-3′ (for GGT-Iβ), respectively. The second PCR was conducted using the respective product of the first reaction as a template. To amplify the GGT-Iα protein-coding region (excluding the stop codon) flanked by a *Bam*HI site (italicized) and the ribosome-binding site (underlined), a sense primer, 5′-GGA*GGATCC*CATGGAAGAAGACGAAGAAATCACATTTG-3′ (primer 1) and an antisense primer, 5′-AAGTTAAAACTCCTCATGATTAGTAATTTTTGTTAAATACCAATCCC-3′ were used. To amplify the GGT-Iβ sequence including the stop codon, flanked by the ribosome-binding site (underlined) and a *Hin*dIII site (italicized), a sense primer, 5′-GAGGAGTTTTAACTTATGAATGCACCTAATTTAAGAAGTGAAG-3′, and an antisense primer, 5′-CCA*AAGCTT*TCAAAGATATGATGGTTTTTCAATTCC-3′ (primer 2), were used. The third round of PCR was conduced using a mixture of the products of the second round, and primers 1 and 2. The resulting 2-kb PCR product was digested with *Bam*HI and *Hin*dIII and ligated into *Bam*HI, and *Hin*dIII double-digested pQE31 (QIAGEN, Hilden, Germany) to construct pEhGGT-Iαβ. Nucleotide sequences were confirmed with an ABI Prism BigDye terminator cycle sequencing ready reaction kit (PE Applied Biosystems, Foster City, CA) on an ABI Prism 310 Genetic Analyzer. In pEhGGT-Iαβ, the GGT-Iα and GGT-Iβ protein-coding regions placed in tandem were presumably translationally coupled, facilitating the co-expression of these two subunits at similar levels. An amino-terminal histidine tag was also engineered in pEhGGT-Iα to facilitate purification.

2.6. Construction of plasmids to express recombinant small GTPases

Construction of plasmids for *Eh*Rasl-4 and *Eh*RacC were previously described [26]. Similarly, a protein-coding region of *Eh*RacA, *Eh*RacG, and *Eh*Rapl-2 flanked by additional *Bam*HI and *Sal*I sites (italicized) were amplified by PCR using cDNA as a template and the following sense and antisense primers: 5′-GGA*GGATCC*CATGCAAGCTGTCAAATGTGT-3′ and 5′-CCAGT*CGAC*TTAGAATAATAAACATCCTCT-3′ (*Eh*RacA); 5′-GGA*GGATCC*CATGAGACCAGTGAAACTTGT-3′ and 5′-CCA*GTCGAC*TTAGAATAATGAGCATCCTTT-3′ (*Eh*RacG); 5′-GGA*GGATCC*CATGCCAGTAAAAGACTATAAAATTGTAGTA-3′ and 5′-CCA*GTCGAC*TTAGAGAAGAGAACAATGATGAGCATGATC-3′ (*Eh*Rapl); 5′-GGA*GGATCC*CATGCCAGTGAAAGACTACAAAATTGTAGTA-3′ and 5′-CCA*GTCGAC*TTAGAAGAGAGAACATCCACCACTCTTCTT-3′ (*Eh*Rap2), where the restriction sites are italicized. PCR products were electrophoresed, purified, and cloned into *Bam*HI, and *Sal*I double-digested pQE31 plasmid to obtain pEhRacA, pEhRacG, pEhRapl and pEhRap2. The resulting plasmids were designed to express proteins containing an amino-terminal histidine tag to facilitate purification.

2.7. Expression and purification of recombinant proteins

Plasmids constructed as described above were introduced into *Escherichia coli* M15 cells. A 12 ml seed culture was grown overnight at 37 °C in LB medium containing 100 μg/ml ampicillin and 25 μg/ml kanamycin. The overnight culture was then inoculated into 250 ml of fresh medium containing the antibiotics. The bacteria were grown for 1 h, and then for another 4 h after the addition of 1 mM isopropyl β-D-thiogalactopyranoside to induce protein expression. The bacteria were harvested by centrifugation at 4000 × *g* for 20 min, and the pellet was stored at −20 °C until purification. The recombinant proteins were purified according to the manufacturers' instructions. Briefly, the bacterial cells were resuspended in cold lysis buffer, phosphate-buffered saline (PBS), pH 8.0, containing 10 mM imidazole and 1% lysozyme, sonicated, and centrifuged at 10,000 × *g* for 20 min. The supernatant was applied to a Ni-NTA agarose column (QIAGEN), washed extensively with the wash buffer containing 20 mM imidazole, and eluted with the lysis buffer containing 250 mM imidazole. The purified recombinant GGT-I and small GTPase proteins were then dialyzed against the enzyme assay buffer described below and 40 mM Tris–HCl, pH 8, containing 90 mM NaCl, 10 mM $MgCl_2$ and 2 mM dithiothreitol (DTT) and stored with 20 and 50% glycerol, respectively, at −80 °C until use. After purification, recombinant *Eh*GGT-I was estimated to be >95% pure by densitometric quantitation. Protein concentrations were determined by the method of Bradford [32] using Protein Assay CBB solution (Nacalai Tesque, Kyoto, Japan). Bovine serum albumin was used as the protein standard.

2.8. Sequence analysis

GGT-Iβ and FTβ protein sequences from *E. histolytica* and 16 other organisms were retrieved from the databases available at TIGR and the National Center for Biotechnology Information (http://www.ncbi.nih.gov/) using the BLASTP and TBLASTN algorithms. The protein alignment and phylogenetic analyses were performed with CLUSTAL W version 1.81 [33] using the Neighbor-joining (NJ) method [34] with the Blosum matrix created using the CLUSTAL W program [33]. Unrooted NJ trees

were drawn with TreeView version 1.6.0 [35]. Branch lengths and bootstrap values (1000 replicates) [36] were derived from the NJ analysis.

2.9. Protein analyses

The expression and purity of recombinant proteins were evaluated by standard sodium dodecyl sulfate-polyacrylamide gel electrophoresis (SDS-PAGE) as described [37]. To prepare *E. histolytica* extracts, trophozoites were washed three times with ice cold PBS, resuspended at 10^7 ml^{-1} in PBS containing a proteinase inhibitor cocktail [1 mM phenylmethylsulfonyl fluoride, 1 nM trypsin inhibitor, 100 μM trans-epoxysuccinyl-L-leucylamino-(4-guanidino) butane, 1 μg/ml pepstatin A, 1 μg/ml leupeptin, 1 μg/ml *N*-α-p-tosyl-L-lysine chloromethyl ketone hydrochloride, and 1 mM benzamidine hydrochloride], and subjected to three cycles of freezing and thawing. After centrifugation at 10,000 × *g* for 10 min, the supernatant was subjected to further analyses.

2.10. Immunoblot analysis

SDS-PAGE was conducted using 4 μg each of recombinant *Eh*GGT-I, *Eh*FT, and recombinant rat GGT-I. Polyclonal antiserum against recombinant *Eh*GGT-I was commercially raised in a rabbit by Takara-Bio (Ohtsu, Japan) by four injections of 0.8 mg of the purified recombinant protein with Freund's complete and incomplete adjuvant at 2-week intervals. Two weeks after the last immunization, the immune serum was collected. Immunoblot analysis was performed as described [37] using primary antibodies at 1:100 and peroxidase-conjugated anti-rabbit IgG antibody (ICN-Cappel, Cappel, OH) at 1:1000. The blots were visualized with 4-chloro-l-naphthol and hydrogen peroxide.

2.11. Enzyme assays

The enzymatic activity of recombinant GGT-I and the whole lysate of *E. histolytica* trophozoites were assayed by measuring the incorporation of [^{3}H] GGPP or [^{3}H] FPP into the recombinant small GTPases of *E. histolytica*, human H-Ras-CVLL, or H-Ras-CVLS. The assay was performed essentially as described previously [38] with minor modifications. Briefly, in standard assays, the reaction mixture contained, in a total volume of 50 μl, 50 mM HEPES, pH 7.5, 5 mM $MgCl_2$, 25 μM $ZnCl_2$, 5 mM DTT, 0.1% PEG 20,000, 130 nM [^{3}H] GGPP (3 μCi/ml) or 187 nM [^{3}H] FPP (3 μCi/ml), 1.8 μg (1.8 μM) of the acceptor, and 2.4 μg (0.6 μM) of the purified recombinant GGT-I or 140 μg of the *E. histolytica* lysate. The reaction was initiated by the addition of either the recombinant enzyme or cell extracts, was run at 30 °C for 20 min, and terminated by the addition of 200 μl of 10% HCl in ethanol. The quenched reactions were allowed to stand at room temperature for 15 min. After the addition of 200 μl of 100% ethanol, the reactions were vacuum-filtered through a glass filter GF/C (Whatman, Maidstone, UK) using a Sampling Manifold (Millipore Corporation, Bedford, MA). The filters were washed with 4 ml of absolute ethanol, and then subjected to scintillation counting (LS 6000IC, Beckman Coulter, Fullerton, CA). The K_m values were calculated from Lineweaver–Burk plots. GGT-I assays were also conducted in the presence of known peptidomimetic inhibitors of GGT-I (GGTI-287 and GGTI-297) under the conditions described above.

3. Results

3.1. Features of GGT-Iβ from E. histolytica

A nucleotide sequence of *Eh*GGT-Iβ obtained by PCR was identical to the sequence available from the genome database (40.m00215). The predicted protein-coding region of *Eh*GGT-Iβ, consisting of 1014 bp, encodes a protein of 337 amino acids with a calculated molecular mass of 38.2 kDa and a p*I* of 6.71. A search for previously identified domains and motifs [39] using the NCBI Conserved Domain Search revealed that *Eh*GGT-Iβ possessed one CAL1 domain and two "prenyltransferase and squalene oxidase repeats" (Fig. 1). The deduced protein sequence of *Eh*GGT-Iβ was aligned with those of other organisms using the CLUSTAL W program (Fig. 1). *Eh*GGT-Iβ is the smallest in size, and apparently lacks the secretory signal sequence, organelle targeting signals, and domains implicated in membrane association including the transmembrane domain and myristoylation signal. *Eh*GGT-Iβ revealed a 22–30% positional identity with the GGT-Iβ of *Saccharomyces cerevisiae*, *Caenorhabditis elegans*, *Drosophila melanogaster*, *Homo sapiens*, or *Arabidopsis thaliana*. Among 12 residues implicated in making contact with peptide substrates in mammalian GGT-Iβ [40], four important residues Ala^{123}, Met^{124}, Arg^{202}, and Leu^{320} in *Hs*GGT-Iβ, were replaced by Ser^{107}, Tyr^{108}, Ser^{189}, and Met^{304}, respectively, in *Eh*GGT-Iβ, (Fig. 1). Furthermore, among 17 residues implicated in making contact with isoprenoid in mammalian GGT-Iβ [40], five residues, Phe^{52}, Thr^{127}, Cys^{177}, Phe^{324}, and Asn^{345} of *Hs*GGT-Iβ, were replaced by Met^{47}, Ala^{111}, Ser^{164}, Cys^{308}, and Il^{329}, respectively, in *Eh*GGT-Iβ (Fig. 1). All three residues implicated in the interaction with zinc in the catalytic center of mammalian GGT-Iβ [40] were conserved in *Eh*GGT-Iβ.

3.2. Phylogenetic analysis of EhGGT-Iβ and EhFTβ

A phylogenetic tree of GGT-Iβ and FTβ from *E. histolytica* and other organisms was constructed (Fig. 2). The β subunit of GGT-I and FT formed statistically significant (i.e. supported with 100% bootstrap proportion) well-separated clades, suggesting that the separation of GGT-I and FT occurred prior to the separation of these species. The β subunit of amebic GGT-I is divergent from those from all the other organisms including mammals; the overall shapes of these two trees are, however, significantly different. These results indicate that the catalytic β subunits of *Eh*FT and *Eh*GGT-I evolved independently to gain phylogenetic positions well separate from other eukaryotes, consistent with the presence of the unique biochemical properties of *Eh*GGT-I (see below).

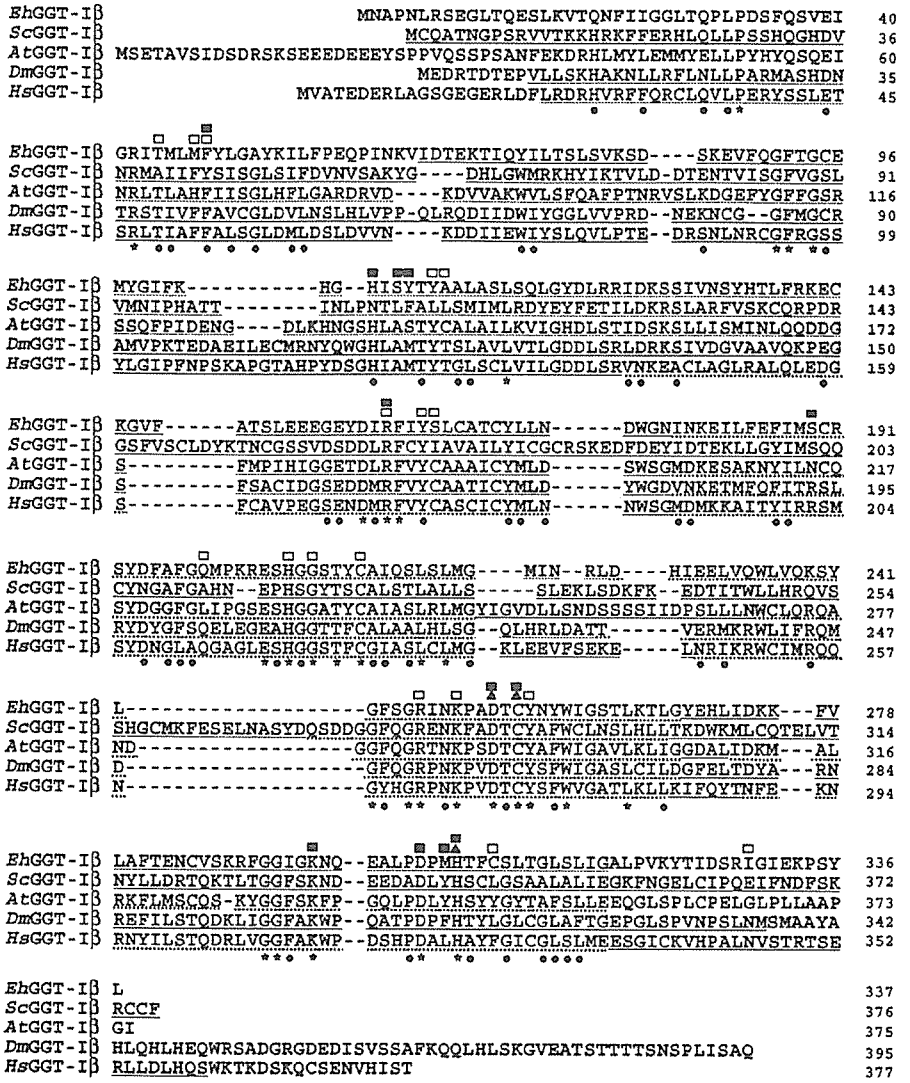

Fig. 1. Alignment of the deduced amino acid sequences of the β subunit of protein geranylgeranyltransferase I from *Entamoeba histolytica* and other organisms. *Eh, E. histolytica; Sc, Saccharomyces cerevisiae; At, Arabidopsis thaliana; Dm, Drosophila melanogaster; Hs, Homo sapiens*. The *asterisks* (*) under the alignments indicate identical amino acid residues and the *dots* (●) indicate conserved amino acid substitutions. CAL1 domains detected by the NCBI Conserved Domain Search are *underlined* (partially *dotted-underlined*). The prenyltransferase/squalene oxidase repeats, also detected by the search, are *dotted-underlined*. Amino acids implicated in the binding of isoprenoids or peptide substrates [40] are marked with *open* or *filled squares*, respectively. Amino acids implicated in the coordination of zinc are marked with *filled triangles*. DDBJ/EMBL/GeneBank™ accession numbers are given in Fig. 2.

3.3. Demonstration of GGT activity of the recombinant EhGGT-I against human Ras proteins

*Eh*GGT-Iα, identical to the previously characterized *Eh*FTα [26], and *Eh*GGT-Iβ were co-expressed in *E. coli*, and the complex was co-purified as described in Section 2. The purified complex revealed two major proteins of an equal intensity with an apparent molecular mass of 38 and 36 kDa on SDS-PAGE analysis (Fig. 3). Although the apparent molecular mass of the recombinant α subunit agreed well with the theoretical value of 37.6 kDa (of the native protein) with the amino- and carboxyl-terminal addition of Met-Arg-Gly-Ser-His-His-His-His-His-His-Thr-Asp-Pro and Gly-Gly-Phe, respectively, β subunit of 36 kDa was smaller than the theoretical value of 38.2 kDa for *Eh*GGT-Iβ. The molecular identity of these two subunits was confirmed using immunoblot analysis (see below). Densitometric quantitation of these two bands also supported the premise that they contain an equal number of protein molecules (data not shown). Thus, the recombinant *Eh*GGT-Iα and *Eh*GGT-Iβ were present as a stable complex with a stoichiometric ratio of 1:1 in the process of purification by Ni-nitrilotriacetic acid (NTA) agarose (Fig. 3). A rabbit antiserum raised against the recombinant *Eh*GGT-I reacted with both the α and β subunits of *Eh*GGT-I and the α subunit of *Eh*FT, but neither with the β subunit of *Eh*FT nor rat GGT-I (Fig. 3B and C). These data confirmed the identity of *Eh*GGT-Iα

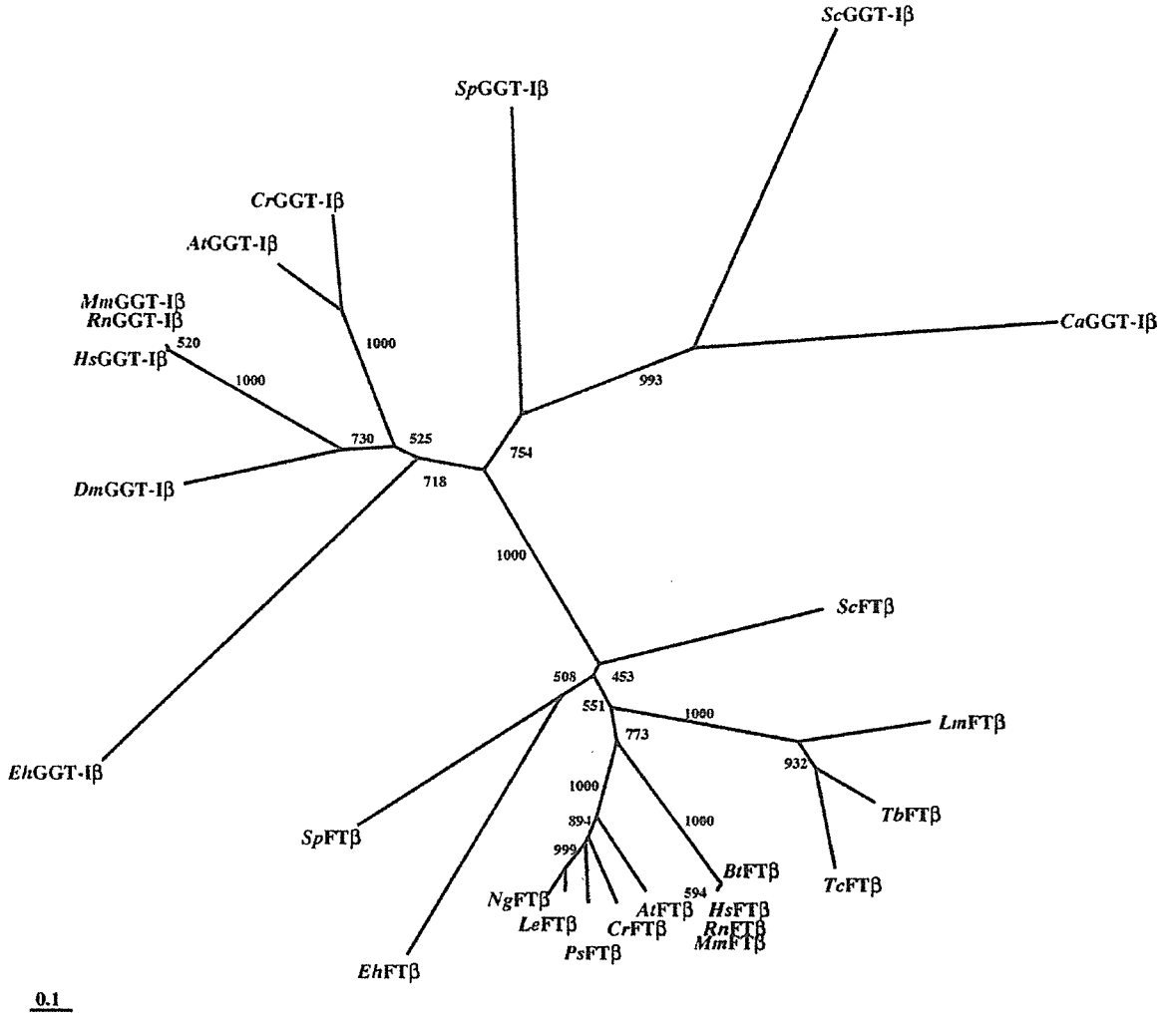

Fig. 2. Phylogenetic tree of the β subunits of GGT-I and FT. The tree was constructed by neighbor-joining distance analysis using the CLUSTAL W and TreeView programs. Line lengths indicate distances between nodes. The bar represents a distance of 0.1 amino acid change per site. Bootstrap values for 1000 replicates are shown at the nodes. Abbreviations are: *Eh, E. histolytica* (DDBJ/EMBL/GeneBank™ number of FTβ and GGT-Iβ, BAC98942, AB161971); *Sc, S. cerevisiae* (P22007, P18898); *Sp, Schizosaccharomyces pombe* (013782, P32434); *Tb, Trypanosoma brucei* (AAF73920, none); *Tc, T. cruzi* (AAL69905, none); *Lm, Leishmania major* (AAL69907, none); *At, A. thaliana* (AAF74564, NP_81487); *Ng, Nicotiana glutinosa* (AAB38796, none); *Ps, Pisum sativum* (Q04903, none); *Le, Lycopersicon esculentum* (AAC49666, none); *Cr, Catharanthus roseus* (AAQ02809, AAP50511); *Ca, Candida albicans* (none, AAD32539); *Dm, D. melanogaster* (none, AAC46972); *Mm, Mus musculus* (NP_666039, NP_766215) *Rn, Rattus norvegicus* (Q02293, P53610); *Bt, Bos taurus* (P49355, none); *Hs, H. sapiens* (NP_002019, NP_005014).

and *Eh*GGT-Iβ to the two corresponding bands on SDS-PAGE. They also suggest that antigenicity differed between the β subunits of *Eh*GGT-I and *Eh*FT and between *Eh*GGT-I and rat GGT-I.

Recombinant *Eh*GGT-I showed comparable GGT activity against both wild-type human recombinant H-Ras-CVLS [1.36 ± 0.028 (mean ± standard deviation of the mean) nmol GGPP/mg protein] and mutant H-Ras-CVLL (1.65 ± 0.013 nmol GGPP/mg protein), whereas rat GGT-I showed activity of a similar level against H-Ras-CVLL (1.83 ± 0.162), but no detectable activity against H-Ras-CVLS (Fig. 4), suggesting the presence of marked differences in acceptor specificity between *E. histolytica* and rat GGT-I.

3.4. Specificities of EhGGT-I for acceptors and prenyl donors

We further examined the acceptor (i.e. protein substrate) specificity of *Eh*GGT-I toward amebic small GTPases, *Eh*Ras, *Eh*Rac, and *Eh*Rap. We tested if *Eh*GGT-I utilizes a limited range of substrates among possible small GTPases, as previously demonstrated for *Eh*FT, which showed very strict substrate specificity predominantly against *Eh*Ras4-CVVA [26]. The recombinant *Eh*GGT-I showed GGT activity toward all the tested *Eh*Ras proteins: *Eh*Rasl-CIMF, *Eh*Ras2-CELL, *Eh*Ras3-CSVM, and *Eh*Ras4-CVVA, with *Eh*Ras2 being the best substrate (Fig. 4). Notable differences in GGT-I activity exist depending upon the Ras species. For example, GGT-I activity

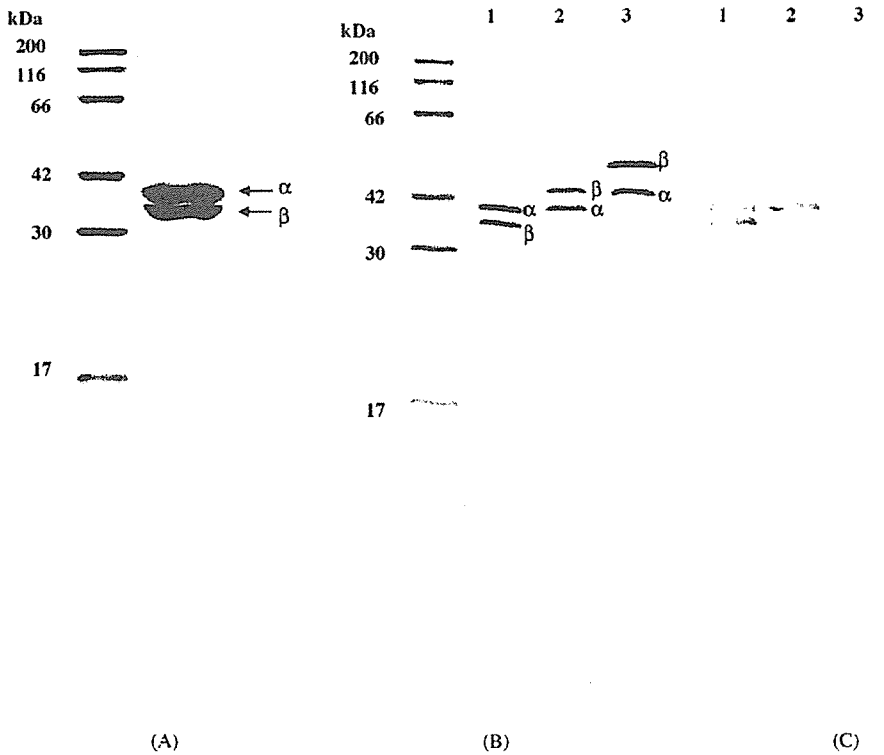

Fig. 3. SDS-PAGE and immunoblot analyses of the purified recombinant GGT-I of *E. histolytica*. (A) *Eh*GGT-1α and β subunits were coexpressed in *Escherichia coli* and purified on Ni-NTA agarose. The samples were subjected to SDS-PAGE and stained with Coomassie Brilliant Blue. (B) Approximately 4 μg each of recombinant *Eh*GGT-I (*Lane* 1), *Eh*FT (*Lane* 2) and rat GGT-I (*Lane* 3) were subjected to SDS-PAGE and stained with Coomassie Brilliant Blue. (C) The same samples in (B) were subjected to SDS-PAGE, transferred, and immunostained with rabbit antiserum against recombinant. *Eh*GGT-I.

toward *Eh*Ras2-CELL was >100 times higher than *Eh*Ras3-CSVM. The recombinant *Eh*GGT-I also transferred geranylgeranyl to *Eh*RacA-CLLF, *Eh*RacC-CALL, *Eh*RacG-CSLF, *Eh*Rapl-CSLL, and *Eh*Rap2-CSLF (Fig. 4). In contrast, rat GGT-I revealed comparable activity against *Eh*RacA-CLLF, *Eh*RacG-CSLF; however, rat GGT-I showed almost no detectable activity against the other three *Eh*Ras proteins and significantly lower activity against *Eh*RacC-CALL, *Eh*Rapl-CSLL, and *Eh*Rap2-CSLF. We also assayed for GGT activity in the whole lysate of the *E. histolytica* trophozoites. GGT activity (4.9–9.4 pmol GGPP/mg protein) was detected against *Eh*Ras 1-4 and human H-Ras-CVLL in the whole lysate, verifying the presence of GGT activity against these representative Ras proteins (data not shown).

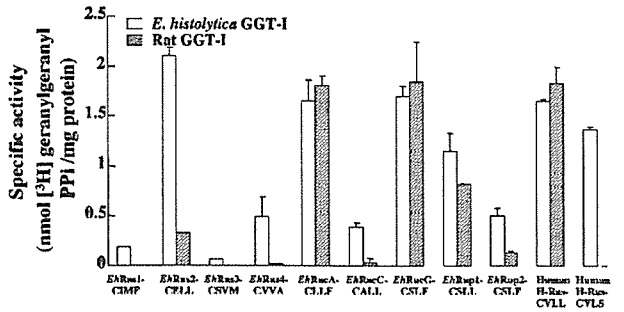

Fig. 4. Protein substrate specificity of recombinant GGT-I of *E. histolytica*. The specific activity of the recombinant *Eh*GGT-I was determined by the incorporation of [^{3}H] geranylgeranyl pyrophosphate into the recombinant *Eh*Ras1-4, *Eh*Rac A, C, G, *Eh*Rapl, 2, wild-type H-Ras-CVLS, and mutant H-Ras-CVLL. The reaction mixture (50 μl) contained 50 mM HEPES, pH 7.5, 5 mM $MgCl_2$, 25 μM $ZnCl_2$, 5 mM DTT, 0.1% PEG 20,000, 130 nM [^{3}H] GGPP (3 μCi/ml), 1.8 μg (1.8 μM) of an acceptor, and 2.4 μg (0.6 μM) of the purified recombinant GGT-I. Means ± standard errors of quadruplicates are shown. DDBJ/EMBL/GeneBank™ accession numbers of these proteins are: *Eh*Rasl, AAA21446; *Eh*Ras2, AAA21447; *Eh*Ras3, BAD07406; *Eh*Ras4, BAB07407; *Eh*RacA, Q24814; *Eh*RacC, Q24816; *Eh*RacG, O76321; *Eh*Rapl, AAA21444; *Eh*Rap2, AAA21445; H-Ras-CVLS, P01112.

We examined the specificity of the prenyl donors of *Eh*GGT-I and rat GGT-I. The recombinant *Eh*GGT-I showed farnesyl transferase activity against *Eh*Ras2-CELL and H-Ras-CVLL at about 27% the efficiency of geranylgeranyltransferase. In contrast, rat GGT-I showed significantly lower FT activity against the same acceptors (3.3–6.6% of GGT-I activity) (data not shown).

3.5. Kinetic properties of EhGGT-I

Lineweaver-Burk plots showed the K_m of recombinant *Eh*GGT-I for *Eh*Ras2 and H-Ras-CVLL to be 0.85 ± 0.11 and 0.2 ± 0.01 μM (plots not shown), respectively. The K_m of recombinant rat GGT-I for H-Ras-CVLL was 6 times higher (1.2 μM [41]), suggesting the higher substrate affinity of the amebic GGT-I toward protein acceptors. *Eh*GGT-I showed a K_m of 0.20 ± 0.05 μM for GGPP (using H-Ras-CVLL as a protein substrate), which is four times lower than that of rat GGT-I

Table 1
Inhibition of recombinant GGT-I from *Entamoeba histolytica* and rat by peptidomimetics

Inhibitors	IC_{50} (μM)			
	E. histolytica GGT-I		Rat GGT-I	
	*Eh*Ras2-CELL	H-Ras-CVLL	*Eh*Ras2-CELL	H-Ras-CVLL
GGTI-287	5.5 ± 1.8	25.3 ± 7.6	0.063 ± 0.004	0.049 ± 0.02
GGTI-297	3.2 ± 0.4	2.1 ± 0.3	0.033 ± 0.004	0.257 ± 0.03

The reaction mixture contained, in a total volume of 50 μl, 50 mM HEPES, pH 7.5, 5 mM $MgCl_2$, 25 μM $ZnCl_2$, 5 mM DTT, 0.1% PEG 20,000, 130 nM [^{3}H] GGPP (3 μCi/ml), 1.8 μg (1.8 μM) of the acceptor, and 2.4 μg (0.6 μM) of the recombinant GGT-I. IC_{50} of each peptidomimetics was determined by measuring specific activities with a range of 0.01–100 μM of the compounds.

(0.81 ± 0.27 μM). *Eh*GGT-I also showed a higher affinity for FPP than rat GGT-I; the K_m of *Eh*GGT-I or rat GGT-I for FPP using H-Ras-CVLL was 29.8 ± 3.7 or >400 nM, respectively.

3.6. Sensitivity of recombinant EhGGT-I to inhibitors of mammalian GGT-I

We examined the sensitivity of *Eh*GGT-I to known peptidomimetic GGT-I inhibitors. As shown in Table 1, *Eh*GGT-I was eight and 516 times more resistant to GGTI-287 than rat GGT-I when recombinant *Eh*Ras2-CELL and H-Ras-CVLL were used as substrates, respectively. *Eh*GGT-I was also 97 and eight times less sensitive to GGTI-297 than rat GGT-I, respectively.

4. Discussion

In this study, we demonstrated marked biochemical differences in the major prenyl enzyme responsible for the lipid modification of Ras and Rho/Rac small GTPases between the enteric protozoan parasite and its mammalian host. This study represents the first biochemical characterization of GGT-I from unicellular protozoa. Our genome-wide search of a GGT-Iβ gene among parasitic protozoa, together with the previous report on the lack of GGT-I activity in kinetoplastids [9], indicates that all protozoan parasites except for *E. histolytica* where the genome database is available lack GGT-I, reinforcing the peculiarity of *E. histolytica*, which possesses both FT and GGT-I. This apparent redundancy of the isoprenylation pathways may be associated with unique features of functions and regulations of Ras/Rap and Rho/Rac proteins through unusual lipid modifications in this parasite. It is totally unknown why *E. histolytica* mainly utilizes GGT-I for lipid modification of a majority of Ras/Rap and Rho/Rac and employs FT for isoprenylation of a very limited subset of Ras isotypes (solely *Eh*Ras4), while the other parasitic protists possess only FT and are likely to have lost GGT-I during parasitic or non-parasitic evolution.

Phylogenetic analyses indicate that *Eh*GGT-Iβ, as well as *Eh*GGT-Iα (*Eh*FTα) in our previous study [26], is only distantly associated with homologues from other organisms. This may partially explain why the unique biochemical properties of the amebic GGT-I that are not shared by its mammalian counterpart exist (see below). Our previous study suggested that α and β subunits of FT co-evolved at a comparable rate among organisms because the phylogenetic trees of the two FT subunits were almost identical [26]. However, the phylogenetic relationship of the β subunit of GGT-I is apparently distinct from that of α and β subunits of FT, refuting a hypothesis of the co-evolution of these two isoprenylation enzymes (Fig. 2).

The results of the GTPase substrate specificity of *Eh*GGT-I indicate that the Ras, Rac, and Rap proteins possessing CaaL, CaaF, CaaM, CaaA, or CaaS at the carboxyl terminus, either from *E. histolytica* or humans, can serve as acceptors for *Eh*GGT-I. Thus, the amebic GGT-I utilizes a broad range of small GTPases for geranylgeranylation. This is in striking contrast to the farnesylation of small GTPases by *Eh*FT, which showed an extremely limited substrate range; only *Eh*Ras4 can serve as a farnesyl acceptor. Our database analysis showed that *E. histolytica* Ras/Rap, Rho/Rac, and Rab with the CaaX terminus possess terminal Leu (42%), Phe (32%), Val (13%), Cys/Met (4% each), or Ala/Ser/Ile (2% each) (data not shown). In mammals, small GTPases with Leu and Val are exclusively geranylgeranylated by GGT-I, and those with Met, Gln, Ser, Ala, Thr, or Cys (in the order of frequency) are solely farnesylated by FT, while those with Phe are modified by both enzymes [42]. In contrast to the amebic GGT-I, mammalian GGT-I does not geranylgeranylate small GTPases with terminals Ala and Ser. Thus, the unique geranylgeranlylation of these small GTPases possessing terminal Ala or Ser in the ameba may confer a unique role to these GTPases. *E. histolytica* small GTPases with the CaaX terminus shows deviation toward Phe at the X position as shown above. However, amebic FT cannot utilize small GTPases terminating with Phe [26]. Taken together, this enteric protozoon strongly relies on GGT-I. It is conceivable that there are biological selections toward the current predominant utilization of GGT-I in this organism. For instance, since the farnesylation of CENP-E, a centromere-associated protein playing a critical role in cell cycle progression in mammals [43], is not present in *E. histolytica*, its modifying enzyme is not required because the isoprenylation of most of small GTPases, except for *Eh*Ras4, is accomplished by GGT-I and GGT-II (Rab GGT, Kumagai, M., Makioka, A., Takeuchi, T. and Nozaki, T., unpublished).

A comparison of ternary complexes of mammalian GGT-I and FT revealed that acceptor specificity is partially determined by surface complementarity between the X residue and the "specificity pocket," to which the side chain of the X residue binds [40]. For instance, the hydrophobic "specificity pocket" discriminates against polar side chains. In addition, the shape and volume of the "specificity pocket" further restrict the range of amino acids most preferably to Leu for GGT-I [40]. However, this preference for Leu was not observed for *Eh*GGT-I. It is intriguing that while the amebic GGT-I prefers *Eh*Ras2-CELL to the other three isotypes of *Eh*Ras possessing Phe, Met, or Ala at the carboxyl terminus (4–33 times in specific activity), it showed an opposite preference for Rac with carboxyl-terminal Phe (*Eh*RacA and *Eh*RacG) over Leu (*Eh*RacC). This observed discrepancy on the acceptor preference of the amebic GGT-I is not artifactual since FT revealed a reverse preference (i.e. approximately eight times higher activity against *Eh*Rasl than

*Eh*Ras2; [26]). These data suggest that the acceptor specificity of the amebic GGT-I is strongly influenced by neighboring residues of GGT-I other than the carboxyl terminus or tertial structure of small GTPases, which is remarkably different from mammalian GGT-I [42]. The data also indicate that the interaction between the surface of GGT-I and the upstream hyper variable region of small GTPases may differ between ameba and mammals. Although the carboxyl terminus of both *Eh*Rasl and *Eh*Ras2 is highly charged (the 17-a.a. carboxyl-terminal region contain nine or seven positively-charged and three or two negatively-charged amino acids in *Eh*Rasl or *Eh*Ras2, respectively), the total polarity of the carboxyl terminus of *Eh*Rasl is significantly higher than *Eh*Ras2. These changes may produce steric differences that lead to changes in substrate specificity. Note that the four substitutions among 12 residues implicated to bind a peptide substrate in mammalian GGT-Iβ [40] (Ala^{123} to Ser^{107}, Met^{124} to Tyr^{108}, Arg^{202} to Ser^{189}, and Leu^{320} to Met^{304}) in *Eh*GGT-Iβ result in the emergence of two hydroxyl-containing residues and the loss of one positive amino acid. The tertial structure of mammalian GGT-I revealed that Ala^{123} and Met^{124} in mammalian GGT-I do not directly interact with X residue of the protein substrate [42], but position close to the X residue. It is conceivable that substituting these amino acids with hydroxyl-containing Ser and aromatic Tyr, respectively, significantly influences the shape and charge of the end of the protein substrate-binding pocket, which likely results in the wider specificity of the amebic GGT-I for protein substrates.

*Eh*GGT-I also utilizes a wider range of isoprenyl donors. *Eh*GGT-I showed four to nine times higher farnesyltransferase activity than rat GGT-I. Five out of 17 residues implicated in the binding of isoprenoid in mammalian GGT-Iβ [40] are substituted in *Eh*GGT-Iβ (Fig. 1). Among these five substitutions (Phe^{52} to Met^{47}, Thr^{127} to Ala^{111}, Cys^{177} to Ser^{164}, Phe^{324} to Cys^{308}, and Asn^{345} to Ile^{329}) in *Eh*GGT-Iβ, Phe^{324} to Cys^{308} is worth noting. Phe^{324} of rat GGT-Iβ is in close proximity to the end of the C20 geranylgeranyl chain and is partially responsible, together with Thr^{49} (also conserved in *Eh*GGT-Iβ), for allowing rat GGT-I to accommodate GGPP in the catalytic pocket [40]. It is conceivable that Phe^{324} to Cys^{308} substitution creates additional water-mediated or non-mediated hydrogen bonds with neighboring residues, which result in the ability of *Eh*GGT-Iβ to utilize FPP as well as GGPP. This substitution may also influence the stability of the enzyme-product complex and the binding of fresh isoprenoid diphosphate to displace the prenyl-peptide product from the active site during the reaction cycle, as shown for rat GGT-I [40].

The amebic GGT-I revealed notable resistance to peptidomimetics known to inhibit mammalian GGT-I (Table 1). This apparent insensitivity of the amebic GGT-I to the inhibitors is not due to the impurity of our preparations since mixing our recombinant GGT-I with rat GGT-I did not influence the inhibition of rat GGT-I by these peptidemimetics. In addition, both amebic and rat GGT-I revealed comparable sensitivity against a GGPP derivative, 3-aza-2,3-dihydro-la-homo-GGPP (kindly donated by Prof. R.M. Coates, University of Illinois) (IC_{50}, approximately 4–10 μM), confirming the observed insensitivity of *Eh*GGT-I against GGTI-287 and GGTI-297. GGTI-287 and GGTI-297 are CaaL peptidomimetics, where reduced C is linked to Leu by 2-phenyl-4-aminobenzoic acid or by 2-naphthyl-4-aminobenzoic acid [44–46]. It is puzzling why the amebic GGT-I is insensitive to these CaaL peptidomimetics because *Eh*GGT-I shows wide donor specificity as discussed above.

Together with our previous study [26], this study indicates that most small GTPases with the CaaX motif from *E. histolytica* are geranylgeranylated or farnesylated by GGT-I, but not farnesylated by FT, which significantly differs from mammals where Ras and Rho/Rac proteins with CaaX are either farnesylated by FT or geranylgeranylated by GGT-I at a comparable frequency [42]. Thus, GGT-I is biologically and physiologically very important for *E. histolytica*, making *Eh*GGT-I an attractive, rational target for the development of new chemotherapeutics against amebiasis.

Acknowledgements

The authors thank Naohiro Watanabe, Jikei, for his valuable discussion and Yumiko Saito-Nakano, NIID, for immunoblotting and her helpful discussion. We also thank Tomomi Yamashita, Jikei, for her technical assistance. This work was supported by a Grant for Precursory Research for Embryonic Science and Technology (PRESTO), Japan Science and Technology Agency to T.N., a Health Sciences Research Grant for Research on Emerging and Re-emerging Infectious Diseases from the Ministry of Health, Labor, and Welfare to A.M. and T.N., Grant-in-Aid for Scientific Research from the Ministry of Education, Culture, Sports, Science and Technology of Japan to A.M. (13670256) and T.N. (16044250, 16017307, 15590378), and a Grant for the Project to Promote Development of Anti-AIDS Pharmaceuticals from the Japan Health Sciences Foundation to T.N. The database search was conducted with the 9× *E. histolytica* genome database available at the Institute for Genomic Research (TIGR) and the Sanger Institute with financial support from the National Institute of Allergy and Infectious Diseases and The Wellcome Trust.

References

[1] Zhang FL, Casey PJ. Protein prenylation: molecular mechanisms and functional consequences. Annu Rev Biochem 1996;65:241–69.
[2] Takai Y, Kaibuchi K, Kikuchi A, Kawata M. Small GTP-binding proteins. Int Rev Cytol 1992;133:187–230.
[3] Boguski MS, McCormick F. Proteins regulating Ras and its relatives. Nature 1993;366:643–54.
[4] Casey PJ, Seabra MC. Protein prenyltransferases. J Biol Chem 1996;271:5289–92.
[5] Maurer-Stroh S, Washietl S, Eisenhaber F. Protein prenyltransferases. Genome Biol 2003;4(212):1–9.
[6] James GL, Goldstein JL, Brown MS. Polylysine and CVIM sequences of K-RasB dictate specificity of prenylation and confer resistance to benzodiazepine peptidomimetic in vitro. J Biol Chem 1995;270:6221–6.
[7] Cox A, Der CJ. Farnesyltransferase inhibitors and cancer treatment: targeting simply Ras? Biochem Biophys Acta 1997;1333:F51–71.
[8] Gibbs JB. Ras C-terminal processing enzymes-new drug targets? Cell 1991;65:1–4.
[9] Gelb MH, Van Voorhis WC, Buckner FS, et al. Protein farnesyl and *N*-myristoyl transferases: piggy-back medical chemistry targets for the

development of antitrypanosomatid and antimalarial therapeutics. Mol Biochem Parasitol 2003;126:155–63.
[10] Sebti SM, Hamilton AD. Farnesyltransferase and geranylgeranyltransferase I inhibitors and cancer therapy: lessons from mechanism and bench-to-bedside translational studies. Oncogene 2000;19:6584–93.
[11] Stark Jr WW, Blaskovich MA, Johnson BA, et al. Inhibiting geranylgeranylation blocks growth and promotes apoptosis in pulmonary vascular smooth muscle cells. Am J Physiol 1998;275:L55–63.
[12] World Health Organization. *Entamoeba* taxonomy, vol. 75. Bull World Health Organ; 1997. pp. 291–292.
[13] Shen P-S, Lohia A, Samuelson J. Molecular cloning of *ras* and *rap* genes from *Entamoeba histolytica*. Mol Biochem Parasitol 1994;64:111–20.
[14] Shen P-S, Sanford JC, Samuelson J. *Entamoeba histolytica*: isoprenylation of $p21^{ras}$ and $p21^{rap}$ in vitro. Exp Parasitol 1996;82:65–8.
[15] Lohia A, Samuelson J. Molecular cloning of a *rho* family gene of *Entamoeba histolytica*. Mol Biochem Parasitol 1993;58:177–80.
[16] Lohia A, Samuelson J. Heterogeneity of *Entamoeba histolytica rac* genes encoding $p21^{rac}$ homologues. Gene 1996;173:205–8.
[17] Ghosh SK, Samuelson J. Involvement of $p21^{racA}$, phosphoinositide 3-kinase, and vacuolar ATPase in phagocytosis of bacteria and erythrocytes by *Entamoeba histolytica*: suggestive evidence for coincidental evolution of amebic invasiveness. Infect Immun 1997;65:4243–9.
[18] Guillen N, Sansonetti P. Rac G, a small GTPase, regulates capping of surface receptors in *Entamoeba histolytica*. Arch Med Res 1997;28:129–31.
[19] Guillen N, Boquet P, Sansonetti P. The small GTP-binding protein RacG regulates uroid formation in the protozoan parasite *Entamoeba histolytica*. J Cell Sci 1998;111:1729–39.
[20] Temesvari LA, Harris EN, Stanley Jr SL, Cardelli JA. Early and late endosomal compartments of *Entamoeba histolytica* are enriched in cysteine proteases, acid phosphatase and several Ras-related Rab GTPases. Mol Biochem Parasitol 1999;103:225–41.
[21] Juarez P, Sanchez-Lopez R, Ramos MA, Stock RP, Alagon A. Rab8 as a molecular model of vesicular trafficking to investigate the latter steps of the secretory pathway in *Entamoeba histolytica*. Arch Med Res 2000;31:S157–9.
[22] Saito-Nakano Y, Nakazawa M, Shigeta Y, Takeuchi T, Nozaki T. Identification and characterization of genes encoding novel Rab proteins from *Entamoeba histolytica*. Mol Biochem Parasitol 2001;116:219–22.
[23] Saito-Nakano Y, Yasuda T, Nakada-Tsukui K, Leippe M, Nozaki T. Rab5-associated vacuoles play a unique role in phagocytosis of the enteric protozoan parasite *Entamoeba histolytica*. J Biol Chem 2004;279:49497–507.
[24] Rodriguez MA, Garcia-Perez RM, Garcia-Rivera G, et al. An *Entamoeba histolytica* Rab-like encoding gene and prote: function and cellular location. Mol Biochem Parasitol 2000;108:199–206.
[25] Loftus B, Anderson I, Davies R, et al. The genome of the protist parasite *Entamoeba histolytica*. Nature 2005;433:865–8.
[26] Kumagai M, Makioka A, Takeuchi T, Nozaki T. Molecular cloning and characterization of a protein farnesyltransferase from the enteric protozoan parasite *Entamoeba histolytica*. J Biol Chem 2004;279:2316–23.
[27] Diamond LS, Mattern CF, Bartgis IL. Viruses of *Entamoeba histolytica* I. Identification of transmissible virus-like agents. J Viol 1972;9:326–41.
[28] Diamond LS, Harlow DR, Cunnick CC. A new medium for the axenic cultivation of *Entamoeba histolytica* and other *Entamoeba*. Trans R Soc Trop Med Hyg 1978;72:431–2.
[29] Nozaki T, Asai T, Kobayashi S, et al. Molecular cloning and characterization of the genes encoding two isoforms of cysteine synthase in the enteric protozoan parasite *Entamoeba histolytica*. Mol Biochem Parasitol 1998;97:33–44.
[30] Higuchi R. Recombinant PCR. In: Innis MA, Gelfand DH, Shinsky JJ, White TJ, editors. PCR Protocols: A Guide to Methods and Applications. New York: Academic Press; 1990. p. 177–83.
[31] Omer CA, Diehl RE, Krai AM. Bacterial expression and purification of human protein prenyltransferases using epitope-tagged, translationally coupled systems. Meth Enzymol 1995;250:3–21.
[32] Bradford MM. A rapid and sensitive method for the quantitation of microgram quantities of protein utilizing the principle of protein-dye binding. Anal Biochem 1976;72:248–54.
[33] Thompson JD, Higgins DG, Gibson TJ. CLUSTAL W: improving the sensitivity of progressive multiple sequence alignment through sequence weighting, position-specific gap penalties and weight matrix choice. Nucleic Acids Res 1994;22:4673–80.
[34] Saitou N, Nei M. The neighbor-joining methods: a new method for reconstructing phylogenetic trees. Mol Biol Evol 1987;4:406–25.
[35] Page RD. TreeView: an application to display phylogenetic trees on personal computers. Comput Appl Biosci 1996;12:357–8.
[36] Felsenstein J. Confidence limits on phytogenies: an approach using the bootstrap. Evolution 1985;39:783–91.
[37] Sambrook J, Fritsch EF, Maniatis T. Molecular Cloning: A Laboratory Manual. Cold Spring Harbor, New York: Cold Spring Harbor Laboratory Press; 1989.
[38] Pompliano DL, Rands E, Schaber MD, Mosser SD, Anthony NJ, Gibbs JB. Steady-state kinetic mechanism of Ras farnesyl:protein transferase. Biochemistry 1992;31:3800–7.
[39] Boguski MS, Murray AW, Powers S. Novel repetitive sequence motifs in the α and β subunits of prenyl-protein transferases and homology of the a subunit to the MAD2 gene product of yeast. New Biologist 1992;4:408–11.
[40] Taylor JS, Reid TS, Terry KL, Casey PJ, Beese LS. Structure of mammalian protein geranylgeranyltransferase type-I. Embo J 2003;22:5063–74.
[41] Zhang FL, Moomaw JF, Casey PJ. Properties and kinetic mechanism of recombinant mammalian protein geranylgeranyltransferase type I. J Biol Chem 1994;269:23465–70.
[42] Reid TS, Terry KL, Casey PJ, Beese LS. Crystallographic analysis of caax prenyltransferases complexed with substrates defines rules of protein substrate selectivity. J Mol Biol 2004;343:417–33.
[43] Abrieu A, Kahana JA, Wood KW, Cleveland DW. CENP-E as an essential component of the mitotic checkpoint in vitro. Cell 2000;102:817–26.
[44] Lerner EC, Qian Y, Hamilton AD, Sebti SM. Disruption of oncogenic K-Ras4B processing and signaling by a potent geranylgeranyltransferase I inhibitor. J Biol Chem 1995;270:26770–3.
[45] McGuire TF, Qian Y, Vogt A, Hamilton AD, Sebti SM. Platelet-derived growth factor receptor tyrosine phosphorylation requires protein geranylgeranylation but not farnesylation. J Biol Chem 1996;271:27402–7.
[46] Qian Y, Vogt A, Vasudevan A, Sebti SM, Hamilton AD. Selective inhibition of type-I geranylgeranyltransferase in vitro and in whole cells by CAAL peptidomimetics. Bioorg Med Chem 1998;6:293–9.